





A Computational Study of the Reaction Cyanoacetylene and Cyano Radical leading to 2-Butynedinitrile and Hydrogen Radical

Emília Valença Ferreira de Aragão^{1,2} , Noelia Faginas-Lago¹ , Marzio Rosi³ , Luca Mancini¹, Nadia Balucani¹ , and Dimitrios Skouteris²

¹ Dipartimento di Chimica, Biologia e Biotecnologie,
Università degli Studi di Perugia, 06123 Perugia, Italy
{emilia.dearagao,luca.mancini2}@studenti.unipg.it
{noelia.faginaslago,nadia.balucani}@unipg.it
² Master-up srl, Via Sicilia 41, 06128, Italy
{emilia.dearagao,d.skouteris}@master-up.it
³ Dipartimento di Ingegneria Civile ed Ambientale,
Università degli Studi di Perugia, 06125 Perugia, Italy
marzio.rosi@unipg.it

Abstract. The present work focuses on the characterization of the reaction between cyanoacetylene and cyano radical by electronic structure calculations of the stationary points along the minimum energy path. One channel, leading to C_4N_2 (2-Butynedinitrile) + H, was selected due to the importance of its products. Using different ab initio methods, a number of stationary points of the potential energy surface were characterized. The energy values of these minima were compared in order to weight the computational costs in relation to chemical accuracy. The results of this works suggests that B2PLYP (and B2PLYPD3) gave a better description of the saddle point geometry, while B3LYP works better for minima.

Keywords: Ab initio calculations, Titan atmosphere, Astrochemistry

1 Introduction

Cyanopolyynes are a family of carbon-chain molecules that have been detected in numerous objects of the Interstellar medium (ISM), such as hot cores, star forming regions and cold clouds [1–4]. They are all linear molecules, with alternating carbon-carbon triple and single bonds. The simplest cyanopolyne, HC_3N , has been among the first organic molecules to be detected in the ISM [5] and up to date also HC_5N , HC_7N , HC_9N and $HC_{11}N$ have been detected at least once in the ISM [6, 7] (the detection of $HC_{11}N$, however, has been recently disputed by Loomis et al. [8] and Cordiner et al. [9]). HC_3N and HC_5N are also abundant in solar-type protostars (see for instance a recent work on IRAS 16293-2422 by

Jaber Al-Edhari et al. [10]).

The shortest and most abundant member of the cyanopolyynes family, HC_3N (cyanoacetylene), is a precursor of chain elongation reactions: the successive addition of C_2H molecules generates the other members of its family, as summarised by Cheikh et al [11]. According to the same authors, however, addition of CN radical instead of C_2H would result in a chain termination reaction by the formation of dicyanopolynes, $\text{NC}(\text{CC})_n\text{CN}$. These species have not been observed in the ISM so far because they lack a permanent electric dipole moment and cannot be detected through their rotational spectrum. However, it has been suggested that they are abundant in interstellar and circumstellar clouds [12]. The recent detection of NCCN [13] via its protonated form NCCNH^+ seems to corroborate the suggestion by Petrie et al. [12]

In 2004, Petrie and Osamura had explored through computational means the formation of C_4N_2 (2-Butynedinitrile) in Titan's atmosphere through many pathways [14]. They had found in particular that the cyano radical addition to cyanoacetylene leads to C_4N_2 . In order to characterize all the stationary points of the potential energy surface, the authors had used at the time the hybrid density functional method B3LYP in conjunction with triple-split valence Gaussian basis set 6-311G** for geometry optimizations and vibrational frequency calculations. Moreover, they had also performed single-point calculations with CCSD(T) in conjunction with aug-cc-pVDZ basis-set, a choice made at the time due to computational costs. As computational power has risen in the last 15 years and new methods have been implemented into quantum chemistry software, more accurate results for the geometries and energies can be obtained.

In our laboratory we have already investigated several reactions of astrochemical interest providing insightful results for the understanding of processes observed in the ISM [15, 16] including those involving or leading N-bearing organic molecules [17–19]. Recently, we have focused on studying the reaction between HC_3N and CN in collaboration with the experimental part of the Perugia group. The preliminary investigation of the potential energy surface of the system $\text{HC}_3\text{N} + \text{CN}$ showed the presence of a number of reactive channels. The search for intermediate and product species always involves the computation of four carbon atoms, two nitrogen atoms and one hydrogen atom, i.e. 39 electrons in total. Ab initio calculations can become prohibitively expensive with a rising number of electrons, therefore a balance between chemical accuracy and computational cost must be reached. The focus of this paper is the exit channel of the reaction between cyanoacetylene and cyano radical that leads to the formation of 2-Butynedinitrile and hydrogen. Four different computational methods were benchmarked in order to check if even cheap methods can get accurate results for this system. A comparison to Petrie and Osamura's results was also done.

The paper is organized as follows: in Sec. 2, the methods and the construction of the potential energy surface are outlined. Preliminary results are reported in Sec. 3 and in Sec. 4 concluding remarks are given.

2 Methods

The Potential Energy Surface (PES) of the system was investigated through the optimization of the most stable stationary points. Following a well established computational scheme [20–26], we optimized the geometry of the stationary points, both minima and saddle points, using a less expensive method with respect to the one employed in order to get accurate energies. Calculations for geometries were performed in order to benchmark three methods: density functional theory, with the Becke-3-parameter exchange and Lee-Yang-Parr correlation (B3LYP) [27,28], Unrestricted-Hartree-Fock (UHF) [29,30], and post Hartree-Fock B2PLYP [31] combined or not with Grimme’s D3BJ dispersion [32,33]. All methods were used in conjunction with the correlation consistent valence polarized basis set aug-cc-pVTZ [34]. In each level of theory, a vibrational frequency analysis was done to confirm the nature of the stationary points: a minimum in the absence of imaginary frequencies and a saddle point if one and only one frequency is imaginary. The assignment of the saddle points was performed using intrinsic reaction coordinate (IRC) calculations [35,36]. Then for each stationary point for all methods, the energy was computed with coupled cluster including single and double excitations and a perturbative estimate of connected triples (CCSD(T)) [37–39]. CCSD(T) is a more accurate method than the ones used for the optimizations, but prohibitive computational costs restricts the use of the method in this particular system to fixed geometry calculations. Finally, zero-point energy correction obtained through the frequency calculations were added to energies obtained from all methods to correct them to 0 K. All calculations were performed using the Gaussian 09 code [40].

3 Results and discussion

The calculation of the different electronic structures shows that the attack of cyano radical on the cyanoacetylene is an energetically favorable process that leads to the formation of an adduct intermediate. Figure 1 gather the geometries at the minimum energy path, starting from the HC_3N and CN reactants and leading to 2-Butynedinitrile and hydrogen. These geometries were optimized at UHF/aug-cc-pVTZ, B3LYP/aug-cc-pVTZ, B2PLYP/aug-cc-pVTZ and B2PLYPD3/aug-cc-pVTZ levels. The reported interatomic distances are in red for UHF, blue for B3LYP and green for both B2PLYP and B2PYLP with Grimme’s D3 dispersion, since no difference in their geometries was recorded. The geometries obtained with the methods above are very similar. The differences between bond lengths and angles are small, with the exception of the transition state geometries. In the saddle point structure, B2PLYP seems to provide a more reasonable distance for weak interaction as the one between carbon and hydrogen: it is 0.162 Å shorter than the distance obtained with B3LYP and 0.241 Å shorter than the one proposed by UHF. B2PLYP is a double-hybrid density functional that combines Becke exchange and Lee, Young and Parr correlation with Hartree-Fock exchange and a perturbative second-order correlation

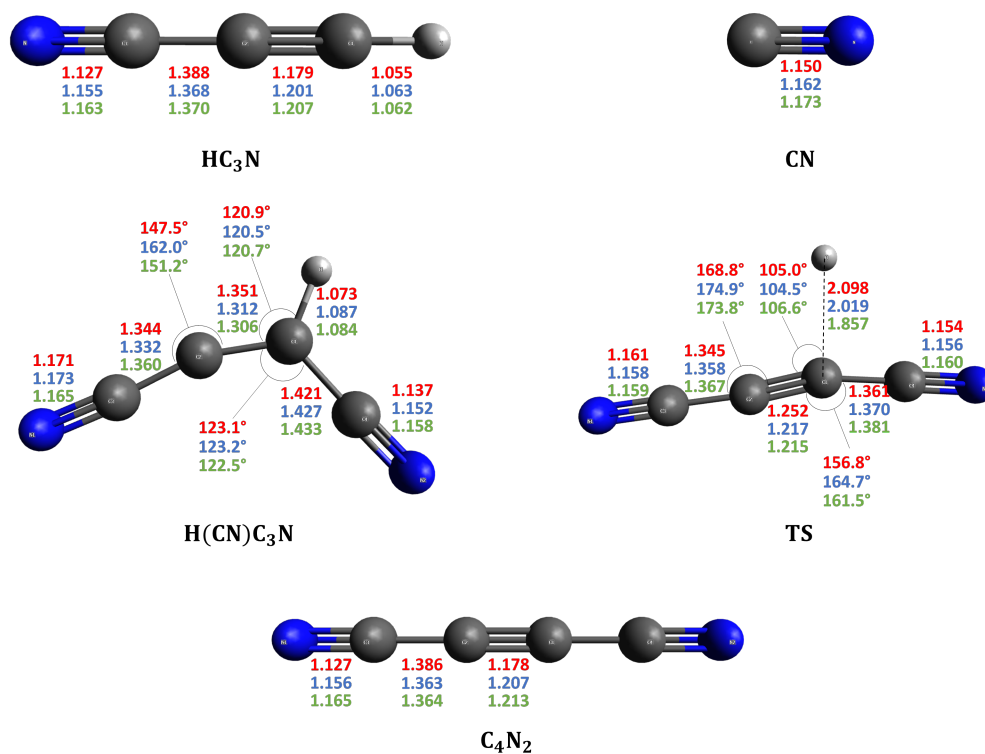


Fig. 1: Optimized geometries of the stationary points along the minimum energy path leading cyanoacetylene and cyano radical to 2-Butynedinitrile and hydrogen. Bond lengths are shown in Å and bond angles are displayed in degrees. UHF values in red, B3LYP values in blue, B2PLYP values in green.

obtained from Kohn-Sham orbitals [31]. According to the author of the method, B2PLYP reports very good results for transition state geometries.

Most of the geometries might be similar, but this does not necessarily mean that all energies also are. Table 1 gathers the relative energies of all geometries computed with every method. The reactants were taken as the reference for the energy. Within the B2PLYP method, the account of Grimme's D3 dispersion changes slightly the energy value, even for an identical geometry. As every method returns different energy values, a direct comparison is not pertinent. However, at least the trend in the evolution of the energies can be compared. First, it can be observed that all stationary points are below the energy of the reactants in all the methods that have been employed. Second, in all methods the adduct intermediate MIN 1 is the most energetically stable structure. In addition, a barrier between the adduct and the products is well characterized for B3LYP and both B2PLYP methods, but it is not the case for the UHF method. Though the saddle point was identified with UHF, the energy of the products

Table 1: Energies ($\text{kJ}\cdot\text{mol}^{-1}$, 0 K) of the different geometries relative to the reactants. The energies are computed at UHF/aug-cc-pVTZ, B3LYP/aug-cc-pVTZ, B2PLYP/aug-cc-pVTZ, and B2PLYPD3/aug-cc-pVTZ levels of theory. In parentheses are the values for the same geometry computed at CCSD(T)/aug-cc-pVTZ level of theory.

	ΔH_0^0 ($\text{kJ}\cdot\text{mol}^{-1}$)			
	UHF (CCSD(T))	B3LYP (CCSD(T))	B2PLYP (CCSD(T))	B2PLYPD3 (CCSD(T))
HC₃N + CN	0.0 (0.0)	0.0 (0.0)	0.0 (0.0)	0.0 (0.0)
MIN 1	-276.6 (-240.8)	-259.0 (-223.8)	-231.7 (-221.0)	-236.2 (-221.0)
TS (MIN 1 \rightarrow C₄N₂ + H)	-62.8 (-50.2)	-65.3 (-44.9)	-48.9 (-25.3)	-53.8 (-25.2)
C₄N₂ + H	-50.3 (-58.7)	-82.7 (-68.1)	-85.6 (-68.1)	-88.0 (-67.9)

returned a higher value. It will be shown, however, that when a single-point energy calculation with these same geometries optimized with UHF is done with the CCSD(T)/aug-cc-pVTZ method, the energy of the products is below the energy of the saddle-point.

In order to compare the geometries optimized with all those methods, single-point CCSD(T) calculations were also performed. The results are reported again in Table 1, in parenthesis. Firstly, it can be observed that the energies of all stationary points, i.e. minima and transition state, are below the energy of the reactants in all the methods used. Secondly, as B2PLYP and B2PLYPD3 optimized geometries were mostly identical, the energies computed with CCSD(T)/aug-cc-pVTZ were also the same. Thirdly, it can be noticed that the energies of the B3LYP optimized geometries are very close to the ones of B2PLYP methods, with the exception of the transition state geometry: for this saddle point, energy difference is around $19.6 \text{ kJ}\cdot\text{mol}^{-1}$. At last, the energies of the UHF optimized geometries are the most different from the others methods. In particular, the energies of the intermediate and transition state gave the lowest energy at CCSD(T) level. In contrast, the energy of the products was the highest one using the UHF geometry. Nevertheless, the energy barrier between the intermediate and the products is now well characterized for all methods.

It is also interesting to look at the barrier height values obtained for each method. Table 2 reports the energy changes and barrier heights, computed at the same levels of theory, for the process leading to 2-Butynedinitrile and hydrogen. The interaction of HC_3N and CN gives rise to the adduct MIN 1 (or $\text{H}(\text{CN})\text{C}_3\text{N}$), more stable than the reactants in all levels of theory. This adduct evolves, through a barrier leading to the transition state, to the products of the reactive channel C_4N_2 and radical H . In all levels of theory, the products are less stable than the adduct. Making a comparison between methods, UHF estimates the largest enthalpy changes and barrier height. UHF is followed by B3LYP, B2PLYPD3 and B2PLYP in this order. In relation to CCSD(T), a higher-level method, UHF and B3LYP energies are systematically overestimated. B2PLYP and B2PLYPD3 overestimates the CCSD(T) in the enthalpy variation attributed

Table 2: Enthalpy changes and barrier height ($\text{kJ}\cdot\text{mol}^{-1}$, 0 K) computed at UHF/aug-cc-pVTZ, B3LYP/aug-cc-pVTZ, B2PLYP/aug-cc-pVTZ, and B2PLYPD3/aug-cc-pVTZ levels of theory. In parentheses are the values for the same geometry computed at CCSD(T)/aug-cc-pVTZ level of theory.

	ΔH_0^\ddagger ($\text{kJ}\cdot\text{mol}^{-1}$)				Barrier height			
	UHF (CCSD(T))	B3LYP (CCSD(T))	B2PLYP (CCSD(T))	B2PLYPD3 (CCSD(T))	UHF (CCSD(T))	B3LYP (CCSD(T))	B2PLYP (CCSD(T))	B2PLYPD3 (CCSD(T))
$\text{HC}_3\text{N} + \text{CN} \rightarrow \text{MIN 1}$	-276.6 (-240.8)	-259.0 (-223.8)	-231.7 (-221.0)	-236.2 (-221.0)				
$\text{MIN 1} \rightarrow \text{C}_4\text{N}_2 + \text{H}$	226.4 (182.1)	176.2 (155.7)	146.0 (152.9)	148.2 (153.1)	213.9 (190.6)	193.6 (178.9)	182.7 (195.7)	182.3 (195.8)

to the formation of the adduct, but underestimate both the barrier and enthalpy change for the reaction that leads the intermediate to the product.

While in this work the aug-cc-pVTZ basis set was employed for every method, Petrie and Osamura [14] carried geometry optimizations at B3LYP level in conjunction with the 6-311G** basis-set and computed the single-point energies at CCSD(T) level in conjunction with aug-cc-pVDZ basis-set. In respect to the geometries obtained, only the transition state and the intermediate geometries were published in their paper. The bond distance and angle values are similar to the ones in the B3LYP/aug-cc-pVTZ optimized geometries. The difference is smaller than when the B3LYP geometries were compared to the ones obtained with other methods. The energies computed at CCSD(T)/aug-cc-pVDZ level are listed in Table 2 of that same paper. Since the authors provided the values of total energy for all stationary points, it was possible to calculate the energy of each point in relation to $\text{HC}_3\text{N} + \text{CN}$. The energy at 0 K is $-231.1 \text{ kJ}\cdot\text{mol}^{-1}$ for the adduct intermediate, $-39.5 \text{ kJ}\cdot\text{mol}^{-1}$ for the transition state and $-58.6 \text{ kJ}\cdot\text{mol}^{-1}$ for the products. The energies of the stationary points are once again below the energy of the reactants. CCSD(T)/aug-cc-pVDZ provides here a lower energy value for the adduct intermediate and a higher energy value for the transition state and the products than CCSD(T)/aug-cc-pVTZ. At $191.6 \text{ kJ}\cdot\text{mol}^{-1}$, the height of the barrier between the adduct intermediate and the products is larger in comparison to CCSD(T)/aug-cc-pVTZ. On the other hand, at $172.5 \text{ kJ}\cdot\text{mol}^{-1}$ the enthalpy change between the adduct and the product is very close to the one showing on Table 2.

4 Conclusions

As far as optimized geometries for stationary points are concerned, the UHF method seems to be inadequate, while DFT methods seem to be more reliable.

In particular, B3LYP functional seems to work well for minima, while better functionals like the B2PLYP seem to be necessary for transition state geometries when van der Waals interactions are present. As far as energies are concerned, however, only more correlated methods like CCSD(T) seems to provide accurate results.

A more general conclusion concerns the reaction mechanism suggested by our calculations, which is also in line with the previous determination by Petrie and Osamura. Similarly to the case of other reactions involving CN and other species holding a triple C–C bond (such as ethyne, propyne and 2-butyne [41–43]), the CN radical interacts with the electron density of triple bond to form an addition intermediate without an activation energy. This is in line with the large value of the rate coefficient derived for the reactions also at very low temperature [11] and makes this process a feasible route of dicyano-acetylene (2-Butynedinitrile) even under the harsh conditions of the interstellar medium.

After completing the derivation of the potential energy surface for the title reaction, we will run kinetic calculations to derive the rate coefficient and product branching ratio. The calculated rate coefficient will be compared with the experimental values derived by Cheikh et al. [11] while the reaction mechanism and product branching ratio will be compared with those inferred by the crossed molecular beam experiments which are now in progress in our laboratory. A thorough characterization of the title reaction will allow us to establish its role in the nitrogen chemistry of the interstellar medium. To be noted that both cyano- and dicyano-acetylene have a strong prebiotic potential [44].

5 Acknowledgements

This project has received funding from the European Union’s Horizon 2020 research and innovation programme under the Marie Skłodowska-Curie grant agreement No 811312 for the project ”Astro-Chemical Origins” (ACO). E.V.F.A. thanks the Dipartimento di Ingegneria Civile ed Ambientale of University of Perugia for allocated computing time. N.F.L. thanks Perugia University for financial support through the AMIS project (“Dipartimenti di Eccellenza-2018–2022”), also thanks the Dipartimento di Chimica, Biologia e Biotecnologie for funding under the program Fondo Ricerca di Base 2017. M.R. acknowledges the project “Indagini teoriche e sperimentali sulla reattività di sistemi di interesse astrochimico” funded with Fondo Ricerca di Base 2018 of the University of Perugia.

References

1. Wyrowski, F., Schilke, P., Walmsley, C.: Vibrationally excited HC_3N toward hot cores. *Astronomy and Astrophysics* **341** (1999) 882–895
2. Taniguchi, K., Saito, M., Sridharan, T., Minamidani, T.: Survey observations to study chemical evolution from high-mass starless cores to high-mass protostellar objects I: HC_3N and HC_5N . *The Astrophysical Journal* **854**(2) (2018) 133

3. Mendoza, E., Lefloch, B., Ceccarelli, C., Kahane, C., Jaber, A., Podio, L., Benedettini, M., Codella, C., Viti, S., Jimenez-Serra, I., et al.: A search for cyanopolyynes in L1157-B1. *Monthly Notices of the Royal Astronomical Society* **475**(4) (2018) 5501–5512
4. Takano, S., Masuda, A., Hirahara, Y., Suzuki, H., Ohishi, M., Ishikawa, S.i., Kaifu, N., Kasai, Y., Kawaguchi, K., Wilson, T.: Observations of ^{13}C isotopomers of HC_3N and HC_5N in TMC-1: evidence for isotopic fractionation. *Astronomy and Astrophysics* **329** (1998) 1156–1169
5. Turner, B.E.: Detection of interstellar cyanoacetylene. *The Astrophysical Journal* **163** (1971) L35–L39
6. Broten, N.W., Oka, T., Avery, L.W., MacLeod, J.M., Kroto, H.W.: The detection of HC_9N in interstellar space. *ApJL* **223** (jul 1978) L105–L107
7. Bell, M., Feldman, P., Travers, M., McCarthy, M., Gottlieb, C., Thaddeus, P.: Detection of HC_{11}N in the cold dust cloud TMC-1. *The Astrophysical Journal Letters* **483**(1) (1997) L61–L64
8. Loomis, R.A., Shingledecker, C.N., Langston, G., McGuire, B.A., Dollhopf, N.M., Burkhardt, A.M., Corby, J., Booth, S.T., Carroll, P.B., Turner, B., Remijan, A.J.: Non-detection of HC_{11}N towards TMC-1: constraining the chemistry of large carbon-chain molecules. *Monthly Notices of the Royal Astronomical Society* **463**(4) (2016) 4175–4183
9. Cordiner, M.A., Charnley, S.B., Kisiel, Z., McGuire, B.A., Kuan, Y.J.: Deep K-band Observations of TMC-1 with the Green Bank Telescope: Detection of HC_7O , Nondetection of HC_{11}N , and a Search for New Organic Molecules. *The Astrophysical Journal* **850**(2) (2017) 187
10. Jaber Al-Edhari, A., Ceccarelli, C., Kahane, C., Viti, S., Balucani, N., Caux, E., Faure, A., Lefloch, B., Lique, F., Mendoza, E., Quenard, D., Wiesenfeld, L.: History of the solar-type protostar IRAS 16293-2422 as told by the cyanopolyynes. *A&A* **597** (2017) A40
11. Cheikh Sid Ely, S., Morales, S.B., Guillemin, J.C., Klippenstein, S.J., Sims, I.R.: Low temperature rate coefficients for the reaction $\text{CN} + \text{HC}_3\text{N}$. *The Journal of Physical Chemistry A* **117**(46) (2013) 12155–12164 PMID: 24047203.
12. Petrie, S., Millar, T., Markwick, A.: NCCN in TMC-1 and IRC+ 10216. *Monthly Notices of the Royal Astronomical Society* **341**(2) (2003) 609–616
13. Agúndez, M., Cernicharo, J., De Vicente, P., Marcelino, N., Roueff, E., Fuente, A., Gerin, M., Guélin, M., Albo, C., Barcia, A., et al.: Probing non-polar interstellar molecules through their protonated form: Detection of protonated cyanogen (NCCNH^+). *Astronomy & Astrophysics* **579** (2015) L10
14. Petrie, S., Osamura, Y.: NCCN and NCCCCN formation in titan’s atmosphere: 2. HNC as a viable precursor. *The Journal of Physical Chemistry A* **108**(16) (2004) 3623–3631
15. Podio, L., Codella, C., Lefloch, B., Balucani, N., Ceccarelli, C., Bachiller, R., Benedettini, M., Cernicharo, J., Faginas-Lago, N., Fontani, F., et al.: Silicon-bearing molecules in the shock L1157-B1: first detection of SiS around a Sun-like protostar. *Monthly Notices of the Royal Astronomical Society: Letters* **470**(1) (2017) L16–L20
16. Skouteris, D., Balucani, N., Ceccarelli, C., Faginas Lago, N., Codella, C., Falcinelli, S., Rosi, M.: Interstellar dimethyl ether gas-phase formation: a quantum chemistry and kinetics study. *Monthly Notices of the Royal Astronomical Society* **482**(3) (2019) 3567–3575

17. Skouteris, D., Balucani, N., Faginas-Lago, N., Falcinelli, S., Rosi, M.: Dimerization of methanimine and its charged species in the atmosphere of Titan and interstellar/cometary ice analogs. *Astronomy & Astrophysics* **584** (2015) A76
18. Balucani, N., Skouteris, D., Ceccarelli, C., Codella, C., Falcinelli, S., Rosi, M.: A theoretical investigation of the reaction between the amidogen, NH, and the ethyl, C_2H_5 , radicals: a possible gas-phase formation route of interstellar and planetary ethanimine. *Molecular Astrophysics* **13** (2018) 30–37
19. Sleiman, C., El Dib, G., Rosi, M., Skouteris, D., Balucani, N., Canosa, A.: Low temperature kinetics and theoretical studies of the reaction $\text{CN} + \text{CH}_3\text{NH}_2$: a potential source of cyanamide and methyl cyanamide in the interstellar medium. *Physical Chemistry Chemical Physics* **20**(8) (2018) 5478–5489
20. Falcinelli, S., Rosi, M., Cavalli, S., Pirani, F., Vecchiocattivi, F.: Stereoselectivity in autoionization reactions of hydrogenated molecules by metastable noble gas atoms: the role of electronic couplings. *Chemistry—A European Journal* **22**(35) (2016) 12518–12526
21. Leonori, F., Petrucci, R., Balucani, N., Hickson, K.M., Hamberg, M., Geppert, W.D., Casavecchia, P., Rosi, M.: Crossed-beam and theoretical studies of the $\text{S}({}^1\text{D}) + \text{C}_2\text{H}_2$ reaction. *The Journal of Physical Chemistry A* **113**(16) (2009) 4330–4339
22. Bartolomei, M., Cappelletti, D., de Petris, G., Teixidor, M.M., Pirani, F., Rosi, M., Vecchiocattivi, F.: The intermolecular potential in NO-N_2 and $(\text{NO-N}_2)^+$ systems: implications for the neutralization of ionic molecular aggregates. *Physical Chemistry Chemical Physics* **10**(39) (2008) 5993–6001
23. de Petris, G., Cartoni, A., Rosi, M., Barone, V., Puzzarini, C., Troiani, A.: The Proton Affinity and Gas-Phase Basicity of Sulfur Dioxide. *ChemPhysChem* **12**(1) (2011) 112–115
24. Leonori, F., Petrucci, R., Balucani, N., Casavecchia, P., Rosi, M., Berteloite, C., Le Picard, S.D., Canosa, A., Sims, I.R.: Observation of organosulfur products (thiovinoxy, thioketene and thioformyl) in crossed-beam experiments and low temperature rate coefficients for the reaction $\text{S}({}^1\text{D}) + \text{C}_2\text{H}_4$. *Physical Chemistry Chemical Physics* **11**(23) (2009) 4701–4706
25. de Petris, G., Rosi, M., Troiani, A.: SSOH and HSSO Radicals: An Experimental and Theoretical Study of $[\text{S}_2\text{OH}]^{0/+/-}$ Species. *The Journal of Physical Chemistry A* **111**(28) (2007) 6526–6533
26. Rosi, M., Falcinelli, S., Balucani, N., Casavecchia, P., Leonori, F., Skouteris, D.: Theoretical Study of Reactions Relevant for Atmospheric Models of Titan: Interaction of Excited Nitrogen Atoms with Small Hydrocarbons. In Murgante, B., Gervasi, O., Misra, S., Nedjah, N., Rocha, A.M.A.C., Taniar, D., Apduhan, B.O., eds.: *Computational Science and Its Applications – ICCSA 2012*, Berlin, Heidelberg, Springer Berlin Heidelberg (2012) 331–344
27. Becke, A.D.: Density functional thermochemistry. III. The role of exact exchange. *The Journal of Chemical Physics* **98**(7) (1993) 5648–5652
28. Stephens, P.J., Devlin, F.J., Chabalowski, C.F., Frisch, M.J.: *Ab Initio* Calculation of Vibrational Absorption and Circular Dichroism Spectra Using Density Functional Force Fields. *The Journal of physical chemistry* **98**(45) (1994) 11623–11627
29. Roothaan, C.C.J.: New developments in molecular orbital theory. *Reviews of modern physics* **23**(2) (1951) 69
30. Pople, J.A., Nesbet, R.K.: Self-consistent orbitals for radicals. *The Journal of Chemical Physics* **22**(3) (1954) 571–572

31. Grimme, S.: Semiempirical hybrid density functional with perturbative second-order correlation. *The Journal of chemical physics* **124**(3) (2006) 034108
32. Grimme, S., Ehrlich, S., Goerigk, L.: Effect of the damping function in dispersion corrected density functional theory. *Journal of computational chemistry* **32**(7) (2011) 1456–1465
33. Goerigk, L., Grimme, S.: Efficient and Accurate Double-Hybrid-Meta-GGA Density Functionals- Evaluation with the Extended GMTKN30 Database for General Main Group Thermochemistry, Kinetics, and Noncovalent Interactions. *Journal of chemical theory and computation* **7**(2) (2011) 291–309
34. Dunning Jr, T.H.: Gaussian basis sets for use in correlated molecular calculations. I. the atoms boron through neon and hydrogen. *The Journal of chemical physics* **90**(2) (1989) 1007–1023
35. Gonzalez, C., Schlegel, H.B.: An improved algorithm for reaction path following. *The Journal of Chemical Physics* **90**(4) (1989) 2154–2161
36. Gonzalez, C., Schlegel, H.B.: Reaction path following in mass-weighted internal coordinates. *Journal of Physical Chemistry* **94**(14) (1990) 5523–5527
37. Bartlett, R.J.: Many-body perturbation theory and coupled cluster theory for electron correlation in molecules. *Annual Review of Physical Chemistry* **32**(1) (1981) 359–401
38. Raghavachari, K., Trucks, G.W., Pople, J.A., Head-Gordon, M.: A fifth-order perturbation comparison of electron correlation theories. *Chemical Physics Letters* **157**(6) (1989) 479–483
39. Olsen, J., Jørgensen, P., Koch, H., Balkova, A., Bartlett, R.J.: Full configuration–interaction and state of the art correlation calculations on water in a valence double-zeta basis with polarization functions. *The Journal of chemical physics* **104**(20) (1996) 8007–8015
40. Frisch, M., Trucks, G., Schlegel, H., Scuseria, G., Robb, M., Cheeseman, J., Scalmani, G., Barone, V., Mennucci, B., Petersson, G., Nakatsuji, H., Caricato, M., Li, X., Hratchian, H.P., Izmaylov, A.F., Bloino, J., Zheng, G., Sonnenberg, J.L., Hada, M., Ehara, M., Toyota, K., Fukuda, R., Hasegawa, J., Ishida, M., Nakajima, T., Honda, Y., Kitao, O., Nakai, H., Vreven, T., Montgomery, J.A.J., Peralta, J.E., Ogliaro, F., Bearpark, M., Heyd, J.J., Brothers, E., Kudin, K.N., Staroverov, V.N., Kobayashi, R., Normand, J., Raghavachari, K., Rendell, A., Burant, J.C., Iyengar, S.S., Tomasi, J., Cossi, M., Rega, N., Milla, J.M., Klene, M., Knox, J.E., Cross, J.B., Bakken, V., Adamo, C., Jaramillo, J., Gomperts, R., Stratmann, R.E., Yazyev, O., Austin, A.J., Cammi, R., Pomelli, C., Ochterski, J.W., Martin, R.L., Morokuma, K., Zakrzewski, V.G., Voth, G.A., Salvador, P., Dannenberg, J.J., Dapprich, S., Daniels, A.D., Farkas, O., Foresman, J.B., Ortiz, J.V., Cioslowski, J., Fox: *Gaussian 09, Revision A. 02*, 2009, Gaussian, Inc., Wallingford CT (2009)
41. Huang, L.C.L., Balucani, N., Lee, Y.T., Kaiser, R.I., Osamura, Y.: Crossed beam reaction of the cyano radical, $\text{CN} (X^2\Sigma^+)$, with methylacetylene, $\text{CH}_3\text{CCH} (X^1\text{A}_1)$: Observation of cyanopropyne, $\text{CH}_3\text{CCCN} (X^1\text{A}_1)$, and cyanoallene, $\text{H}_2\text{CCCHCN} (X^1\text{A}')$. *The Journal of Chemical Physics* **111**(7) (1999) 2857–2860
42. Balucani, N., Asvany, O., Chang, A.H.H., Lin, S.H., Lee, Y.T., Kaiser, R.I., Bettinger, H.F., Schleyer, P.v.R., Schaefer III, H.F.: Crossed beam reaction of cyano radicals with hydrocarbon molecules. II. Chemical dynamics of 1-cyano-1-methylallene ($\text{CNCH}_3\text{CCCH}_2$; $X^1\text{A}'$) formation from reaction of $\text{CN} (X^2\Sigma^+)$ with dimethylacetylene $\text{CH}_3\text{CCCH}_3 (X^1\text{A}_1)$. *The Journal of Chemical Physics* **111**(16) (1999) 7472–7479

43. Huang, L.C.L., Asvany, O., Chang, A.H.H., Balucani, N., Lin, S.H., Lee, Y.T., Kaiser, R.I., Osamura, Y.: Crossed beam reaction of cyano radicals with hydrocarbon molecules. IV. Chemical dynamics of cyanoacetylene (HCCCN ; $X^1\Sigma^+$) formation from reaction of CN ($X^2\Sigma^+$) with acetylene, C_2H_2 ($X^1\Sigma_g^+$). *The Journal of Chemical Physics* **113**(19) (2000) 8656–8666
44. Balucani, N.: Elementary reactions of N atoms with hydrocarbons: first steps towards the formation of prebiotic N-containing molecules in planetary atmospheres. *Chemical Society Reviews* **41**(16) (2012) 5473–5483